Proc. Natl. Acad. Sci. USA
Vol. 76, No. 9, pp. 4170–4174, September 1979
Chemistry

Ligated chlorophyll cation radicals: Their function in photosystem II of plant photosynthesis

(electron spin resonance/monomeric chlorophyll/*P*-680/primary donor/photosynthetic oxygen evolution)

M. S. DAVIS*, A. FORMAN†, AND J. FAJER*

*Department of Energy and Environment and †The Medical Research Center, Brookhaven National Laboratory, Upton, New York 11973

Communicated by Joseph J. Katz, May 17, 1979

ABSTRACT Magnesium tetraphenylchlorin, a synthetic model for chlorophyll, exhibits significant variations in the unpaired spin densities of its cation radicals with concomitant changes in oxidation potentials as a function of solvent and axial ligand. Similar effects are observed for chlorophyll (Chl) a and its cation radicals. Oxidation potentials for Chl → $Chl^{+\cdot}$ as high as +0.9 V (against a normal hydrogen electrode) are observed in nonaqueous solvents, with linewidths of the electron spin resonance signals of monomeric $Chl^{+\cdot}$ ranging between 9.2 and 7.8 G in solution. These changes in electronic configuration and ease of oxidation are attributed to mixing of two nearly degenerate ground states of the radicals theoretically predicted by molecular orbital calculations. Comparison of the properties of chlorophyll *in vitro* with the optical, redox, and magnetic characteristics attributed to *P*-680, the primary donor of photosystem II which mediates oxygen evolution in plant photosynthesis, leads us to suggest that *P*-680 may be a ligated chlorophyll monomer whose function as a phototrap is determined by interactions with its (protein?) environment.

Photosynthesis in algae and green plants functions via two chlorophyll (Chl)-mediated systems that cooperatively oxidize water (photosystem II, PS II) and reduce carbon dioxide (PS I) (1–14). The primary chemical products generated by the light harvested by the antenna network and funnelled to the reaction centers are believed to be oxidized Chls, $P\text{-}700^{+\cdot}$ in PS I and $P\text{-}680^{+\cdot}$ in PS II (1–14), and reduced Chl or pheophytin (11, 15–17). The optical changes associated with the oxidations of *P*-700 and *P*-680 (18–24), particularly an enhanced absorption at ≈820 nm, and the electron spin resonance (ESR) linewidths and *g*-values (10, 24–32) are characteristic of Chl π cation radicals (33). ESR (10, 25–26), ENDOR (electron-nuclear double resonance) (34–35), optical, and circular dichroism (36) results have further established the dimeric or "special pair" nature of $P\text{-}700^{+\cdot}$. ESR data show (25) that the 7 G (1 G = 10^{-4} tesla) peak-to-peak linewidth (ΔH) of $P\text{-}700^{+\cdot}$ is narrower by $\sqrt{2}$ than that of $Chl^{+\cdot}$ (ΔH = 9 G) in dichloromethane and dichloromethane/methanol solutions, as expected if the unpaired electron of the radical is equally shared between two Chl molecules. Additional support for delocalization of spin over two Chls in $P\text{-}700^{+\cdot}$ derives from ENDOR spectra of oxidized chloroplasts (34, 35) in which several proton hyperfine splittings are found to be approximately half those of $Chl^{+\cdot}$ *in vitro* (37, 38). The nature of $P\text{-}680^{+\cdot}$ in PS II is considerably more ambiguous: linewidths of ESR signals attributed to $P\text{-}680^{+\cdot}$ range from 7 to 9 G (27–32), resulting in proposals of monomer (28), dimer (29–31), and even trimer (32) configurations. Even more puzzling are the large differences in oxidation potentials of *P*-700 and *P*-680. Titrations of *P*-700 yield a midpoint potential (39–41) ranging between +0.4 and +0.5 V against the normal hydrogen electrode, whereas the minimum potential needed to oxidize water to oxygen at the physiological pH sets a lower limit of +0.8 V for *P*-680 (2, 4).

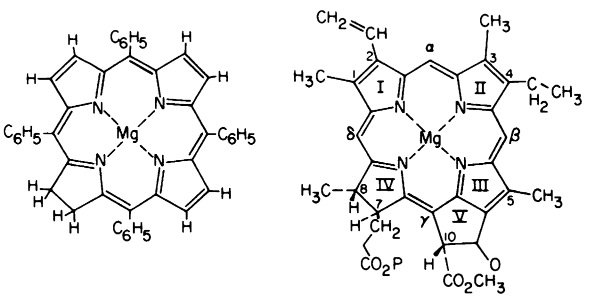

FIG. 1. Structural formulas of MgTPC (*Left*) and Chl a (*Right*).

We describe here *in vitro* magnetic, redox, and optical properties of Chl, of magnesium tetraphenylchlorin (MgTPC, Fig. 1), a model compound, and of their π cation radicals, which illustrate the environmental factors capable of altering the properties of Chl *in vivo*. We find that the oxidation potentials and the ESR and ENDOR characteristics of the chlorins are sensitive functions of solvent and counterion. These environmentally mediated changes may be explained by theoretical calculations that predict the existence of a nearly degenerate excited state whose degree of interaction is influenced by the perturbations caused by the axial ligands—i.e., the immediate environment of the Chl. Comparison of the optical, redox, and magnetic data of the chlorins *in vitro* with those attributed to *P*-680 leads us to propose that *P*-680 is a Chl monomer whose function as the phototrap of PS II is determined by its interactions with its immediate (protein?) surroundings.

EXPERIMENTAL

The techniques used for obtaining ESR, ENDOR, and optical spectra, for solvent purification, and for cyclic voltammetry, controlled-potential electrolyses, and coulometry have been described (42–44). Junction potentials, induced by solvent changes, were estimated by comparing halfwave potentials ($E_{1/2}$) for the oxidation of ferrocene (45) in the solvents under investigation.

Chl a was purified and dried by standard methods (42, 46). Tetraphenylchlorin (H_2TPC), and H_2TPC deuterated at the reduced ring ($[^2H_4]H_2TPC$), were synthesized by the procedure of Whitlock *et al.* (47). Magnesium was inserted by reacting H_2TPC with Grignard reagent (48) and recrystallizing the resulting MgTPC. Combined spectrophotometric and coulometric measurements indicated that oxidation of Chl and

---

Abbreviations: PS, photosystem; ESR, electron spin resonance; ENDOR, electron-nuclear double resonance; $E_{1/2}$, polarographic half-wave potential; Chl, chlorophyll; H_2TPC, tetraphenylchlorin; MgTPC, magnesium tetraphenylchlorin; PrCN, butyronitrile; H_4furan, tetrahydrofuran; SCF-MO, self-consistent-field molecular orbital.

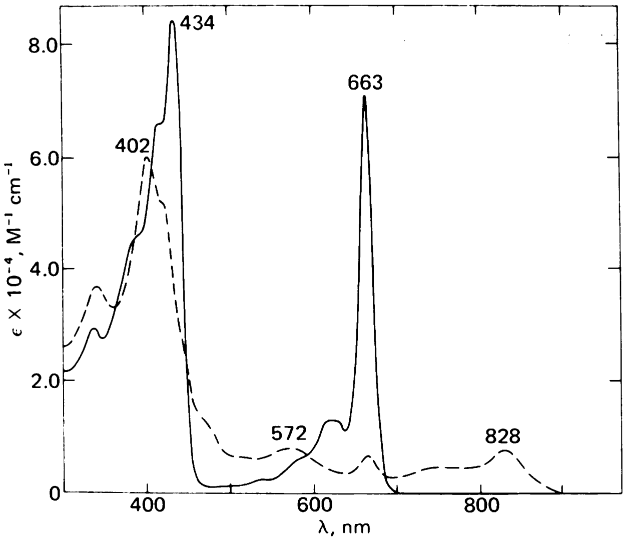

FIG. 2. Optical spectra, at 25°C, in 3:1 CH_2Cl_2/H_4furan, of anhydrous Chl a (——) and its cation radical, $Chl^{+\cdot}ClO_4^-$ (– –).

MgTPC to their respective cations required 1.1 ±0.1 (SEM) electron/chlorin. Reduction of the radicals yielded better than 90% recovery of the starting material.

The cation radicals of Chl and MgTPC used in the ESR studies were generated electrochemically (44) *in situ* at a platinum electrode, with tetrapropyl- or tetrabutylammonium perchlorate as carrier electrolyte, or chemically, by electron transfer (33) to the oxidized salts of zinc tetraphenylporphyrin ($ZnTPP^{+\cdot}ClO_4^-$) and of the μ-oxo-dimer of iron tetraphenylporphyrin [$(FeTPP)_2O^+ClO_4^-$]. $MgTPC^{+\cdot}Cl^-$ was prepared by addition of an excess of tetraethyl ammonium chloride to $MgTPC^{+\cdot}ClO_4^-$.

RESULTS

The spectral changes caused by the one-electron oxidation of Chl in CH_2Cl_2/tetrahydrofuran (H_4furan) mixtures are shown in Fig. 2. The bleaching of the major transitions and the appearance of new bands in the red parallel those found for zinc (33) and magnesium (unpublished results) tetraphenylchlorins and suggest that the changes observed are characteristics of the oxidation of the chlorin π system and, thus, that MgTPC is a reasonable model for Chl. The cation of $MgTPC^{+\cdot}ClO_4^-$ displays a resolved five-line ESR spectrum (Fig. 3) clearly due to four protons with hyperfine splittings, $a_H = 5.6$ G, as shown in the simulation (Fig. 3*b*). This hyperfine interaction can be assigned to the four β protons of the saturated ring of the chlorin by selective deuteration. Substitution of the four protons of that ring by deuterons results in a narrowed ESR spectrum attributable to four deuterons with $a_D = 0.86$ G, as expected because of the differences in gyromagnetic ratios ($a_D/a_H = 0.1535$) and nuclear spins of hydrogen and deuterium and as confirmed by simulation (Fig. 3*d*).

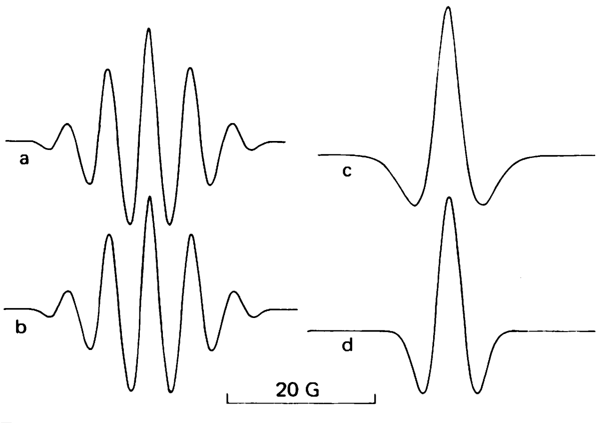

FIG. 3. (*a* and *c*) Second-derivative ESR spectra in CH_2Cl_2 at 25°C ($g = 2.0026$) of $MgTPC^{+\cdot}ClO_4^-$ (*a*) and $[^2H_4]MgTPC^{+\cdot}ClO_4^-$ (saturated ring deuterated) (*c*). (*b* and *d*) Simulations assume four protons with $a_H = 5.63$ G (*b*) and four deuterons, $a_D = 0.86$ G (*d*).

Table 1. Unpaired spin densities for the normal ($^2A_2$) and excited ($^2B_2$) state (for an assumed C_{2v} symmetry)*

$MC^{+\cdot}$			$MC^{+\cdot}$ with vinyl and carbonyl groups	
$^2A_2$	$^2B_2$	Position	$^2A_2$	$^2B_2$
0.008	0.062	21(N)	0.007	0.073
−0.006	0.001	22(N)	−0.003	0.021
−0.012	0.050	23(N)	−0.011	0.028
−0.006	0.001	24(N)	−0.006	0.029
0.138	0.042	1	0.119	0.015
0.138	0.042	4	0.109	0.030
0.002	0.041	5	−0.002	0.140
0.008	0.075	6	0.080	0.000
0.046	0.039	7	0.028	0.069
0.010	0.053	8	0.014	0.021
0.133	0.060	9	0.134	0.019
−0.042	0.087	10	0.038	0.128
0.119	0.032	11	0.121	0.004
0.029	0.015	12	0.032	0.026
0.029	0.015	13	0.029	0.023
0.119	0.032	14	0.125	0.007
−0.042	0.087	15	−0.045	0.130
0.133	0.060	16	0.132	0.016
0.010	0.053	17	0.014	0.017
0.046	0.039	18	0.043	0.029
0.008	0.075	19	0.081	0.002
0.002	0.041	20	0.008	0.117
		25	0.002	0.011
		26	0.011	0.026
		27	−0.002	0.000
		28(O)	0.017	0.013

* Calculated by open shell SCF-MO theory (43, 49) for the cation radicals of a metallochlorin (MC) and a model of Chl a.

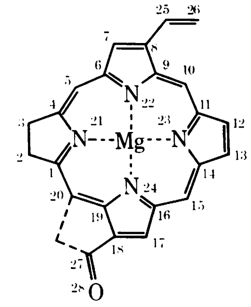

Self-consistent-field molecular orbital (SCF-MO) calculations predict that two nearly degenerate ground states, separated by ≈2000 cm^{-1}, are possible for oxidized chlorins. The calculated spin densities for these states are listed in Table 1. The experimentally observed splitting constant of a β proton is given (38, 49) by $a_H = \rho_c(-9.2 + 96.7 \cos^2\theta)$, in which ρ_c is the spin density on the α-carbon of the π system (C_1 and C_4 in the present case) and θ is the dihedral angle between the $2p_z$ orbital of the α-carbon and the plane defined by C_α, C_β, and H_β. X-ray diffraction studies of single crystals indicate that θ for the β protons of the saturated rings range from an average of 34° in zinc tetraphenylchlorin (38) to 45° in ethylchlorophyllides (50).

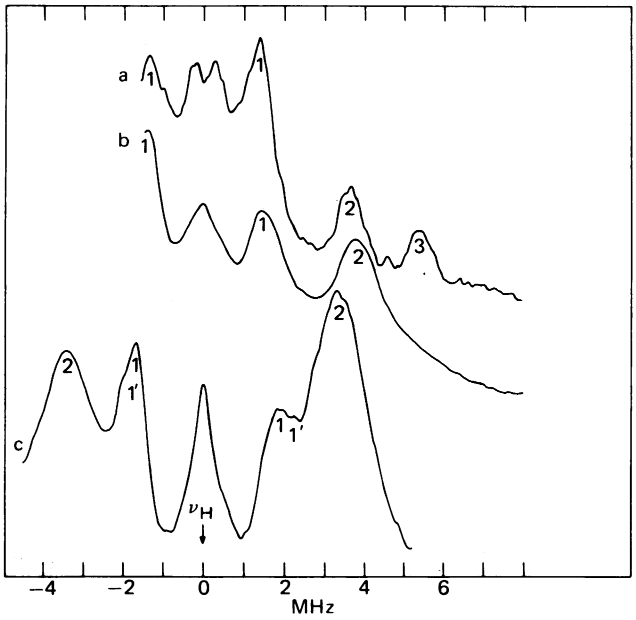

FIG. 4. ENDOR spectra of $\mathrm{Chl}^{+\cdot}\mathrm{ClO_4}^-$ in 1:1 $\mathrm{CH_2Cl_2}$/mineral oil at −30°C (curve a) and −160°C (curve b) and in $\mathrm{H_4}$furan at −160°C (curve c). In curve a, peaks 1, 2, and 3 occur at 1.38, 3.72, and 5.32 MHz and correspond to $a_H/2$. In curve b, peaks 1 and 2 are observed at 1.40 and 3.74 MHz, while in curve c, peaks 1, 1′, and 2 are found at 1.71, 2.01, and 3.38 MHz (2.8 MHz = 1 G). Both high- and lowfield portions of the spectra are shown in curve c. Data are presented relative to the free proton frequency (ν_H = 13.66 MHz).

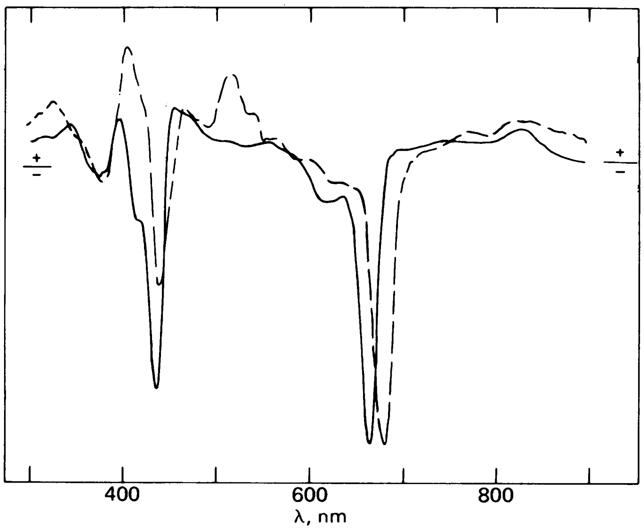

FIG. 5. Comparison of the optical changes induced by light in particles enriched in PS II as reported by Pulles *et al.* (24) (Δ*P*-680, - -) and of the difference spectra obtained (Fig. 2) on oxidation of Chl *in vitro* (ΔChl, —). Solvent, $\mathrm{CH_2Cl_2}$/25% $\mathrm{H_4}$furan. Spectra have been normalized at ≈680 nm.

These values, combined with the predicted spin density of 0.138 for an $^2A_2$ state (Table 1), yield splitting constants, a_H, of 7.9 and 5.4 G (for θ = 34° and 45°) compared with the 5.6 G found experimentally. The magnitude of the β proton splittings observed for $\mathrm{MgTPC}^{+\cdot}\mathrm{ClO_4}^-$ in $\mathrm{CH_2Cl_2}$ is, thus, in general accord with the spin densities predicted for the α carbons of the saturated ring in the $^2A_2$ state.

The electronic configuration of monomeric $\mathrm{Chl}^{+\cdot}$ in $\mathrm{CH_2Cl_2}$ or $\mathrm{CH_2Cl_2/CH_3OH}$, in which the radical exhibits a 9-G linewidth, has been mapped by ENDOR and selective deuteration (Fig. 4 and refs. 37 and 38). The results are also consonant with the $^2A_2$ ground state (assuming an approximate C_{2v} symmetry) predicted by the SCF-MO calculations for a model of $\mathrm{Chl}^{+\cdot}$ (Table 1) and by extended Hückel calculations, which specifically treat the chlorophyll molecule (51). In $\mathrm{CH_2Cl_2}$, the β proton splittings of ring IV (37, 38) are notably smaller in $\mathrm{Chl}^{+\cdot}$ (≈4 G, Fig. 4, curve a, peak 3) than in $\mathrm{MgTPC}^{+\cdot}\mathrm{ClO_4}^-$, as expected for the 45° dihedral angle of the β protons in Chl (50) and the smaller spin densities calculated for the α carbons (Table 1, carbons 1 and 4). The predicted a_H values are 4.6 and 4.3 G.

However, we find that significant variations in the splitting constants of $\mathrm{MgTPC}^{+\cdot}$ can be induced by variations in temperature, solvent, and counterion. At −20°C, a_H = 5.36 G for $\mathrm{MgTPC}^{+\cdot}\mathrm{Cl}^-$ in $\mathrm{CH_2Cl_2}$; a_H = 5.77 G in $\mathrm{CH_2Cl_2}$, 4.50 G in $\mathrm{H_4}$furan, and 3.90 G in butyronitrile (PrCN) for $\mathrm{MgTPC}^{+\cdot}\mathrm{ClO_4}^-$. The difference between $\mathrm{CH_2Cl_2}$ and PrCN is particularly striking; it is over 30%.

A similar effect, reflected in changes of linewidth, is noted with $\mathrm{Chl}^{+\cdot}\mathrm{ClO_4}^-$: ΔH = 9.2 G in $\mathrm{CH_2Cl_2}$, 7.8 G in PrCN, and 7.9 G in $\mathrm{H_4}$furan and $\mathrm{CH_2Cl_2}$/$\mathrm{H_4}$furan at 25°C. That these changes are not due to dimerization is shown by the optical spectra of Chl in these solvents, which are typical of monomeric Chl (52) (see Fig. 2), and by comparison of the ENDOR spectra of $\mathrm{Chl}^{+\cdot}$ in frozen solutions of $\mathrm{CH_2Cl_2}$ and $\mathrm{CH_2Cl_2}$/$\mathrm{H_4}$furan (Fig. 4). Methyl protons, bonded to an α carbon of a π radical, are easily detected by ENDOR at low temperatures because of the combination of favorable relaxation times and small anisotropies (43, 53). This effect is demonstrated in the spectra obtained at −160°C and shown in Fig. 4. The ENDOR transitions observed (peaks 1 and 2) have been assigned to methyl

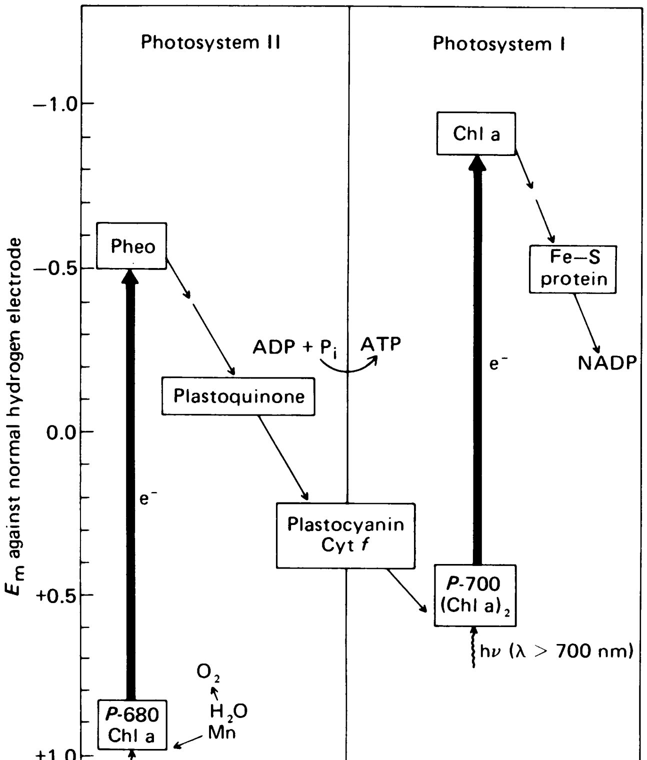

FIG. 6. Revised Z scheme for electron transport of green plant photosynthesis, which incorporates monomeric Chl as the primary donor of PS II and pheophytin and Chl as primary acceptors of PS II and I (11, 14–17). The other species shown in the scheme are discussed in refs. 2 and 4.

Table 2. Half-wave oxidation potentials, $E_{1/2}$ (in V against normal hydrogen electrode)

Solvent	Counterion	MgTPC	Chl a
CH_2Cl_2	ClO_4^-	0.66	0.80
	Cl^-	0.60	0.74
PrCN	ClO_4^-	0.73	0.82
	Cl^-	0.65	0.75
H_4furan	ClO_4^-	0.82	0.93
CH_2Cl_2/5% PrCN	ClO_4^-	0.67	0.81
	Cl^-	0.64	0.75
CH_2Cl_2/5% H_4furan	ClO_4^-	0.74	0.85
	Cl	0.69	0.78

The half-wave potentials are not corrected for junction potentials due to changes in solvent. These effects can be estimated by comparison of the ferrocene/ferricinium couple in the same solvents (45). $E_{1/2}$ for this oxidation is ≈40 mV larger in H_4furan and ≈30 mV smaller in PrCN than in CH_2Cl_2. In mixed solvents, shifts of ±10 mV were found.

groups 1 and 5 on rings I and III, and the assignment was verified by deuteration (37). Note that, although the linewidth of $Chl^{+\cdot}$ in CH_2Cl_2/H_4furan is 8 G, the methyl proton splittings, ≈1.4 and 2.4 G, are close to those found in pure CH_2Cl_2, 1.0 and 2.6 G, and are clearly *not* halved as expected for a dimeric radical. [Peak 1, due to the 1-methyl group, masks transitions due to the methyl and methylene groups on ring II (37). These are partly resolved in the H_4furan spectra (peaks 1 and 1′) and again are consistent with a monomer configuration.] By analogy with the variations in the large β proton splittings found in $MgTPC^{+\cdot}$, we conclude that the variations in linewidth observed in $Chl^{+\cdot}$ are also due to the same proton splittings. Computer simulations of the linewidths of $Chl^{+\cdot}$ in H_4furan or PrCN by using the experimentally determined methyl splittings require a decrease in the splittings of the β protons of ring IV of ≈30% to ≈2.8 G, in agreement with the changes found in $MgTPC^{+\cdot}$ in the same solvents.

The significant interaction of the chlorins with their environment, as reflected in their ESR and ENDOR spectra, is further illustrated by the wide range of oxidation potentials induced by simple changes in solvent[‡] and counterion (Table 2). Again, H_4furan and PrCN, which most profoundly affect the electronic configuration, cause the largest changes in redox potential in the presence of a noncomplexing counterion such as ClO_4^-. Complexation by chloride ion, on the other hand, stabilizes the charge of the cation and thus lowers the oxidation potential.

DISCUSSION

The ESR and redox changes observed for $Chl^{+\cdot}$ and $MgTPC^{+\cdot}$ [similar results are also obtained (38) with $ZnTPC^{+\cdot}$] may reflect mixing of the two nearly degenerate ground states predicted theoretically (Table 1). The $^2B_2$ excited state shows significantly smaller spin densities at the α carbons of the saturated ring than the $^2A_2$ state. If the solvent or counterion induces a sufficient perturbation to mix in some character of the second state, then the splitting constants of the β protons would result in lower values than expected for a pure $^2A_2$. Extended Hückel calculations (ref. 51 and unpublished results) further support this interpretation and actually predict that ligands such as H_2O, CH_3OH, CH_3SH, CH_3CN, and H_4furan would suppress the $^2B_2$ state below the $^2A_2$ in chlorins and Chl. Although this is not observed experimentally, the Hückel and SCF-MO calculations clearly suggest that interactions between the two states are energetically accessible. Changes in the coordination sphere of the chlorins provide a likely mechanism for this mixing. Indeed, resonance Raman and optical spectra indicate that Chl is hexacoordinated in H_4furan and methyl-H_4furan at low temperatures (refs. 52 and 57; M. Lutz, personal communication).

Extension of these results to P-680 leads us to the following conclusions. (*i*) Because reductions in the linewidth of $Chl^{+\cdot}$ can be achieved by changes in solvent, the linewidth alone cannot be used as a rigorous indicator of the structural nature of Chl *in vivo*. Without substantiation by other techniques, such as ENDOR, the ESR results reported for $P\text{-}680^{+\cdot}$ do not, alone, justify the conclusion that it is a dimer. (*ii*) Comparison of the optical difference spectrum ascribed (24) to oxidation of P-680 with that reported here for the oxidation of monomeric Chl in CH_2Cl_2/H_4furan shows reasonable agreement (Fig. 5) if the shift from 670 to 680 nm in P-680 is attributed to a change in coordination of the Chl of P-680, possibly involving nearby protein residues.[§] (*iii*) The oxidation potentials found *in vitro* for monomeric Chl (as high as 0.9 V) approach the limits required for the function of P-680 in oxygen evolution. The optical, magnetic, and redox properties of ligated, monomeric Chl are thus not inconsistent with those attributed to P-680. We suggest, therefore, that P-680 is a monomeric Chl whose physical and chemical characteristics and whose function as the phototrap of photosystem II are determined by its immediate (protein?) environment. We have incorporated this idea and recent postulates (11, 14–17) regarding the primary acceptors of PS I and II into the revised Z scheme shown in Fig. 6 to describe the gross features of electron transport in plant photosynthesis.

We thank Drs. T. Cotton, L. K. Hanson, and M. Lutz for communicating unpublished results, Prof. R. H. Felton for the SCF-MO program, and Dr. L. D. Spaulding for the synthesis of MgTPC. This work was performed under the auspices of the Chemical Sciences Division, U.S. Department of Energy, Washington, DC, under Contract EY76-C-02-0016.

1. Barber, J., ed. (1977) *Primary Processes of Photosynthesis*, (Elsevier, Amsterdam).
2. Govindjee, ed. (1978) *Bioenergetics of Photosynthesis*, (Academic, New York).
3. Knaff, D. B. (1977) *Photochem. Photobiol.* **26**, 327–340.
4. Bearden, A. J. & Malkin, R. (1975) *Q. Rev. Biophysics* **7**, 131–177.
5. Radmer, R. & Kok, B. (1975) *Annu. Rev. Biochem.* **44**, 409–451.
6. Butler, W. L. (1973) *Acc. Chem. Res.* **6**, 177–184.
7. Witt, H. T. (1971) *Q. Rev. Biophys.* **4**, 365–477.
8. Emerson, R. (1956) *Annu. Rev. Plant Physiol.* **9**, 1–24.
9. Hill, R. & Bendall, D. S. (1960) *Nature (London)* **186**, 136–137.
10. Katz, J. J., Norris, J. R., Shipman, L. L., Thurnauer, M. C. & Wasielewski, M. R. (1978) *Annu. Rev. Biophys. Bioeng.* **7**, 393–434.
11. Sauer, K. (1979) *Annu. Rev. Phys. Chem.*, **30**, 155–178.
12. Witt, H. T. (1979) *Biochim. Biophys. Acta* **505**, 355–427.
13. Knaff, D. B. & Malkin, R. (1978) *Curr. Top. Bioenerg.* **7**, 137–175.
14. Ke, B. (1978) *Curr. Top. Bioenerg.* **7**, 76–139.
15. Klimov, V. V., Klevanik, A. V., Shuvalov, V. A. & Krasnovskii, A. A. (1977) *FEBS Lett.* **82**, 183–186.

[‡] Similar variations in the oxidation potentials of Chl have been noted previously (54–56).

[§] We note, for example, that the absorption spectrum of monomeric bacteriochlorophyll is shifted from 775 nm in CH_2Cl_2 to 809 nm in the bacteriochlorophyll-protein complex of *Prosthecochloris aestuarii* strain 2K (58), in which specific bacteriochlorophyll-protein residue interactions are evident from x-ray data (59). Chl-protein binding has also been invoked to explain resonance Raman data on antenna Chl (60).

16. Fujita, I., Davis, M. S. & Fajer, J. (1978) *J. Am. Chem. Soc.* **100,** 6280–6282.
17. Shuvalov, V. A., Dolan, E. & Ke, B. (1979) *Proc. Natl. Acad. Sci. USA* **76,** 770–773.
18. Kok, B. (1956) *Biochim. Biophys. Acta* **22,** 379–401.
19. Ke, B. (1973) *Biochim. Biophys. Acta* **301,** 1–33.
20. Doring, G., Stiehl, H. H. & Witt, H. T. (1967) *Z. Naturforsch.* **22B,** 639–644.
21. Doring, G., Renger, G., Vater, J. & Witt, H. T. (1969) *Z. Naturforsch.* **24b,** 1139–1146.
22. Mathis, P. & Vermeglio, A. (1975) *Biochim. Biophys. Acta* **369,** 371–381.
23. Haveman, J. & Mathis, P. (1976) *Biochim. Biophys. Acta* **440,** 346–355.
24. Pulles, M. P. J., Van Gorkum, H. J. & Verschoor, G. M. (1976) *Biochim. Biophys. Acta* **440,** 98–106.
25. Norris, J. R., Uphaus, R. A., Crespi, H. L. & Katz, J. J. (1971) *Proc. Natl. Acad. Sci. USA* **68,** 625–628.
26. Katz, J. J. & Norris, J. R. (1973) *Curr. Top. Bioenerg.* **5,** 41–75.
27. Malkin, R. & Bearden, A. J. (1975) *Biochim. Biophys. Acta* **396,** 250–259.
28. Goldfield, M. G., Halilov, R. I., Hangulov, S. V., Kononenko, A. A. & Knox, P. P. (1978) *Biochem. Biophys. Res. Commun.* **85,** 1199–1203.
29. Van Gorkum, H. J., Tamminga, J. J. & Haveman, J. (1974) *Biochim. Biophys. Acta* **347,** 417–438.
30. Van Gorkum, H. J., Pulles, M. P. J. & Wessel, J. S. C. (1975) *Biochim. Biophys. Acta* **408,** 331–339.
31. Visser, J. W. M., Rijersberg, C. P. & Gast, P. (1977) *Biochim. Biophys. Acta* **460,** 36–46.
32. Visser, J. W. M. (1975) Dissertation (State Univ., Leiden, The Netherlands).
33. Borg, D. C., Fajer, J., Felton, R. H. & Dolphin, D. (1970) *Proc. Natl. Acad. Sci. USA* **67,** 813–820.
34. Norris, J. R., Scheer, H., Druyan, M. E. & Katz, J. J. (1974) *Proc. Natl. Acad. Sci. USA* **71,** 4897–4900.
35. Feher, G., Hoff, A. J., Isaacson, R. A. & Ackerson, L. C. (1975) *Ann. N.Y. Acad. Sci.* **244,** 239–259.
36. Phillipson, K. D., Sato, V. L. & Sauer, K. (1972) *Biochemistry* **11,** 4591–4605.
37. Scheer, H., Katz, J. J. & Norris, J. R. (1977) *J. Am. Chem. Soc.* **99,** 1372–1381.
38. Fajer, J., Davis, M. S., Brune, D. C., Spaulding, L. D., Borg, D. C. & Forman, A. (1976) *Brookhaven Symp. Biol.* **28,** 74–104.
39. Kok, B, (1971) *Biochim. Biophys. Acta* **48,** 527–532.
40. Evans, M. C., Sihra, C. H. & Slibus, A. R. (1977) *Biochem. J.* **162,** 75–85.
41. Knaff, D. B. & Malkin, R. (1973) *Arch. Biochem. Biophys.* **159,** 552–562.
42. Borg, D. C., Forman, A. & Fajer, J. (1976) *J. Am. Chem. Soc.* **98,** 6889–6893.
43. Fajer, J., Forman, A., Davis, M. S., Spaulding, L. D., Brune, D. C. & Felton, R. H. (1977) *J. Am. Chem. Soc.* **99,** 4134–4140.
44. Fajer, J., Brune, D. C., Davis, M. S., Forman, A. & Spaulding, L. D. (1975) *Proc. Natl. Acad. Sci. USA* **72,** 4596–4660.
45. Bauer, D. & Breant, M. (1975) in *Electroanalytical Chemistry*, ed. Bard, A. J. (Dekker, New York), Vol. 8, pp. 281–348.
46. Strain, H. H. & Svec, W. A. (1966) in *The Chlorophylls*, eds. Vernon, L. P. & Seeley, G. R. (Academic, New York), pp. 21–63.
47. Whitlock, H. W., Hanauer, R., Oester, M. W. & Bower, B. K. (1969) *J. Am. Chem. Soc.* **91,** 7485–7489.
48. Granick, S. (1948) *J. Biol. Chem.* **175,** 333–342.
49. Fajer, J., Borg, D. C., Forman, A., Felton, R. H., Dolphin, D. & Vegh, L. (1974) *Proc. Natl. Acad. Sci. USA* **71,** 994–998.
50. Chow, H. C., Serlin, R. & Strouse, C. E. (1975) *J. Am. Chem. Soc.* **97,** 7230–7237.
51. Hanson, L. K., Davis, M. S., Fujita, I. & Fajer, J. (1978) *Biophys. J.* **21,** 195a.
52. Cotton, T. M., Loach, P. A., Katz, J. J. & Ballschmitter, K. (1978) *Photochem. Photobiol.* **27,** 735–749.
53. Hyde, J. S., Rist, G. H. & Eriksson, L. E. G. (1968) *J. Phys. Chem.* **72,** 4269–4276.
54. Kazakova, A. A., Kiselev, B. A. & Yevstigneyev, V. B. (1976) *Biofizika* **21,** 445–449.
55. Diehn, B. & Seeley, G. R. (1968) *Biochim. Biophys. Acta* **153,** 862–867.
56. Galloway, L., Roettger, J., Fruge, D. R. & Fong, F. K. (1978) *J. Am. Chem. Soc.* **100,** 4635–4638.
57. Hägele, W., Schmid, D., Drissler, F., Naus, J. & Wolf, H. C. (1978) *Z. Naturforsch* **33a,** 1197–1205.
58. Olson, J. M. (1978) in *The Photosynthetic Bacteria*, eds. Clayton, R. K. & Sistrom, W. R. (Plenum, New York), pp. 161–178.
59. Fenna, R. E. & Matthews, B. W. (1976) *Brookhaven Symp. Biol.* **28,** 170–182.
60. Lutz, M. (1977) *Biochim. Biophys. Acta* **460,** 408–430.